Journal Pre-proof

Network Analysis Guided Designing of Multi-Targeted Anti-Fungal Agents: Synthesis and Biological Evaluation

Manmeet Singh , Himanshu Verma , Priyanka Bhandu ,
Manoj Kumar , Gera Narendra , Shalki Choudhary ,
Pankaj Kumar Singh , Om Silakari
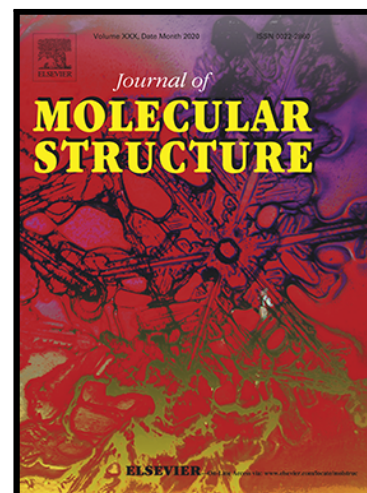
Please cite this article as: Manmeet Singh , Himanshu Verma , Priyanka Bhandu , Manoj Kumar , Gera Narendra , Shalki Choudhary , Pankaj Kumar Singh , Om Silakari , Network Analysis Guided Designing of Multi-Targeted Anti-Fungal Agents: Synthesis and Biological Evaluation, *Journal of Molecular Structure* (2022), doi: https://doi.org/10.1016/j.molstruc.2022.134128

Network Analysis Guided Designing of Multi-Targeted Anti-Fungal Agents: Synthesis and Biological Evaluation

Manmeet Singh[1], Himanshu Verma[1], Priyanka Bhandu[1], Manoj Kumar[1], Gera Narendra[1], Shalki Choudhary[1], Pankaj Kumar Singh[2], Om Silakari*[,1]

[1] *Molecular Modeling Lab (MML), Department of Pharmaceutical Sciences and Drug Research, Punjabi University, Patiala, Punjab, 147002, India.*

[2] *Faculty of Medicine, Integrative Physiology and Pharmacology, Institute of Biomedicine, University of Turku, Turku, FI-20014, Finland*

Corresponding authors; E-mail address: mmlpup73@gmail.com (O.Silakari)

Tel: +91-9501542696: Fax: +91-1752283075

Highlights

- Scaffold hopping approach to optimize reported structure of *N*-(1,3-benzothiazole-2-yl)-2-(pyridine-3-ylformohydrazido) acetamide.
- Network analysis to identify the anti-fungal targets of designed benzothiazole based derivatives.
- Molecular docking and dynamics simulations to understand interaction pattern of designed molecules.
- Synthesis and biological evaluation of optimized structures of *N*-(1,3-benzothiazole-2-yl)-2-(pyridine-3-ylformohydrazido) acetamide.

Abstract

During the ongoing pandemic, there have been increasing reports of invasive fungal disease (IFD), particularly among immunocompromised populations. *Candida albicans* is one of the most common clinical pathogenic microorganisms which have become a serious health threat to population either infected with Covid-19 or on treatment with immunosuppressant's/broad-range antibiotics. Currently, benzothiazole is a well explored scaffold for anti-fungal activity, especially mercapto substituted benzothiazoles. It is reported that exploring the 2nd position of benzothiazoles yield improved anti-fungal molecules. Therefore, in the current study, lead optimization approach using bioisosteric replacement protocol was followed to improve the anti-fungal activity of an already reported benzothiazole derivative, *N*-(1,3-benzothiazole-2-yl)-2-(pyridine-3-ylformohydrazido) acetamide. To rationally identify the putative anti-candida targets of this

derivative, network analysis was carried out. Complexes of designed compounds and identified putative targets were further analyzed for the docking interactions and their consequent retention after the completion of exhaustive MD simulations. Top seven designed compounds were synthesized and evaluated for *in-vitro* anti-fungal property against Candida, which indicated that compounds 1.2c and 1.2f possess improved and comparable anti-fungal activity to *N*-(1,3-benzothiazole-2-yl)-2-(pyridine-3-ylformohydrazido) acetamide and Nystatin, respectively.

Key Words: Network analysis, Molecular docking, Molecular dynamics, 2-aminobenzothiazole

Introduction

The global incidences of fungal infections are rapidly rising among critically sick patients especially in the current pandemic situation (Lia et al. 2020). One of an emerging invasive pathogenic form of fungal yeast is *Candida albicans* which is often regarded as an opportunistic pathogen. The patients with fungal infection and comorbidities accounts for nearly 1.5 million deaths annually which are nearly same as observed with tuberculosis or malaria (Scordino, Giuffrè et al. 2019). The emergence of such a high number of fungus infected cases in ongoing pandemic situation stimulated researchers to come with effective therapeutics that may halt the spread of *C. albicans*. This species is also a commensal of human mucosa (with innate acquired immunity) which remains harmless on the human microbiota (specifically skin, gastrointestinal and genito-urinary mucosal linings) (Lohse et al. 2018). However, during the propitious conditions, an imbalance is created leading to the increased growth of *C. albicans* which causes the infection, as explained in **Fig.1** (Chu et al. 2020). Majorly, disturbances caused by shifts in nutritional alterations, pH, antibiotic use, shifts in oxygen levels, diseases, or immunosuppressant therapy can promote the over-proliferation of C. albicans and observation of their subsequent symptoms (Calderone et al. 2001; Lohse et al. 2018; Pappas et al. 2004; Wenzel et al.1995). In immuno-suppressed individuals such as patients with AIDS, patients undergoing chemotherapy and individuals receiving immunosuppressant therapies are particularly susceptible to systemic infections which are clinically termed as candidiasis (Kullberg et al. 2002, Weig et al. 1998). This results in various type of topical candidiasis including those at mucosa of oral, GIT and genital cavities.
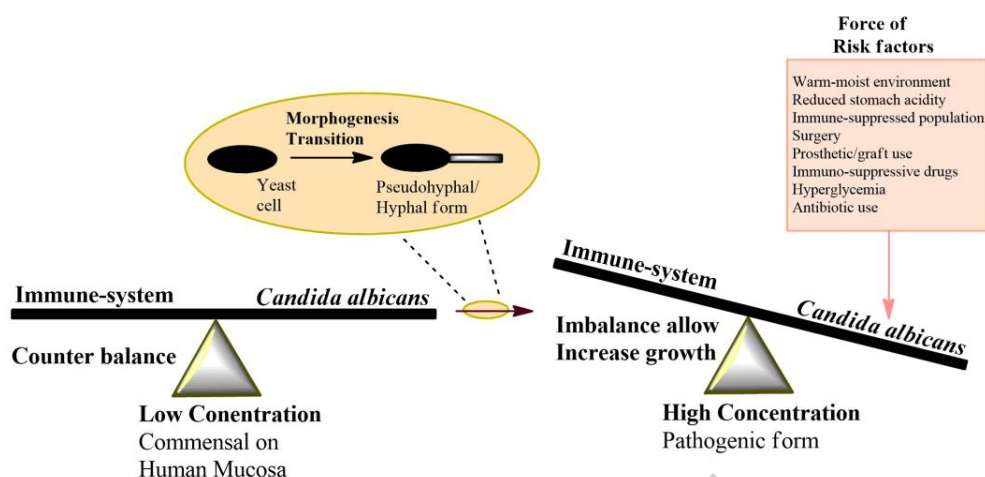
Fig.1. Triggering stimuli for *C. albicans* pathogenicity.

Currently, the use of pre-existing marketed medications mentioned in **Fig.2** for anti-candida activity is limited due to the issues of resistance and unfavorable PK profile (Sheng et al. 2006; Friggeri et al. 2018). The researchers are still making tremendous efforts to develop anti-fungal agent with improved potency and favorable PK profile. Already existing anti-candida leads can also be optimized by different strategies of drug discovery and development process. Lead optimization is a rational approach by which new analogues with improved potency and/or improved pharmacokinetics or reduced toxicity can be designed using systematic structure manipulation of already reported drug candidates (Budha et al. 2008).
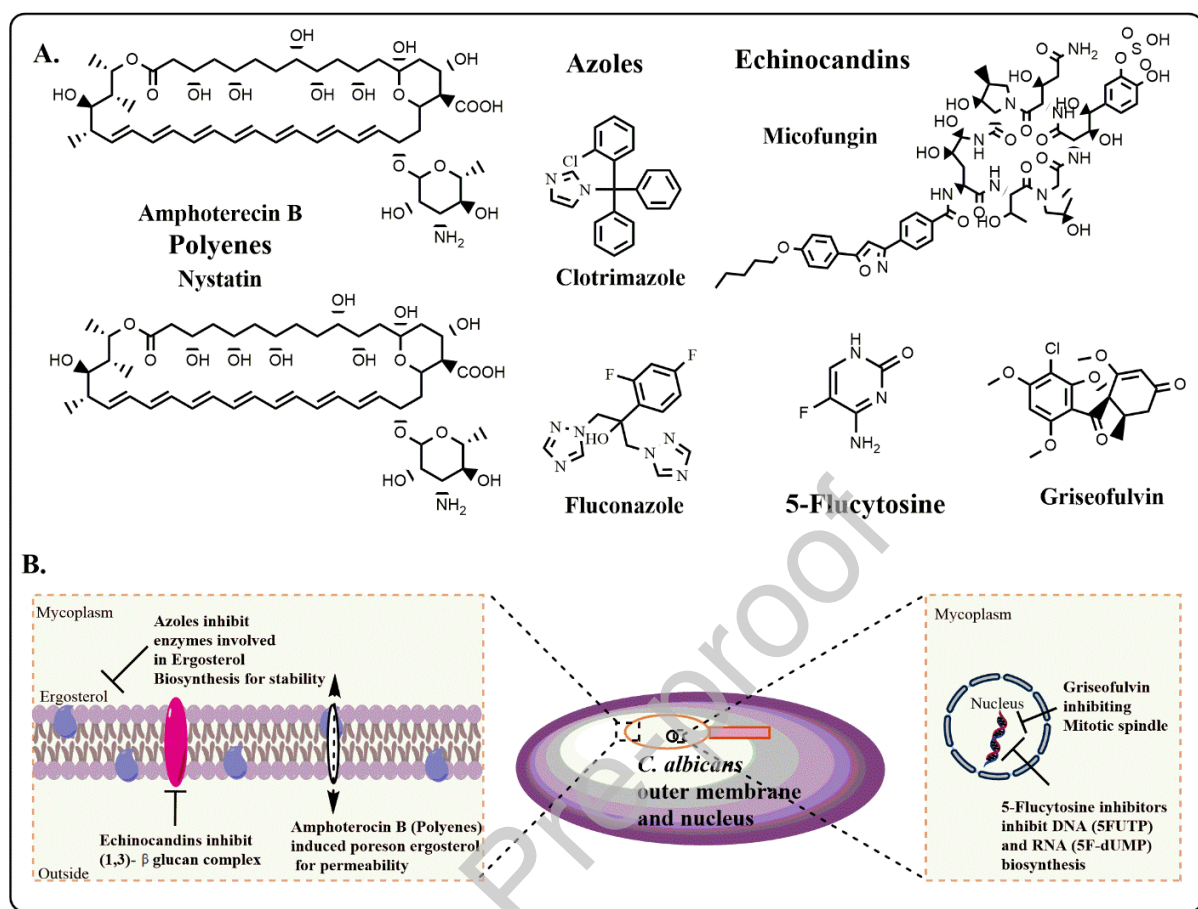
Fig.2. Commercial medication with their chemical structures (A) and the mechanism of anti-fungal action (B).

A number of reports suggested that benzothiazole has also been well explored scaffold for anti-fungal activity, especially with mercapto group at 2nd position of this scaffold (Catalano, Carocci et al. 2013; Amnerkar, Bhongade et al. 2015; Bala, Kumari et al. 2018; Franchini et al., 2009). Since 2-aminobenzothiazole are closest bio-isosteric partner of 2-mercapto-benzothiazole and the most optimum position to explore different substitutions is at 2nd position, it was worthwhile to design the novel molecules of 2-aminobenzothiazole with varied substitution at 2nd position. Later, the variedly substituted derivatives of top scored bioisosteres were rationally searched for their anti-fungal targets using network analysis. To further confirm the potential of these derivatives as anti-fungal agents, structure-based drug designing approaches including molecular docking; electrostatic complementarity and molecular dynamics were implemented.

2. Materials and Methods

2.1. Bioisosteric replacement

Spark module of Cresset performs bioisosteric replacement analysis using "common" and "very common" databases from ZINC drug-like set, ChEMBL, and theoretical rings. These databases include fragments that have been observed 100−500 times or more than 500 times, respectively (Lee et al. 2018). The results are obtained in terms of bioisosteres ranked on the basis of scores including Shape score, BIF%, Score and field score (Spark, version 10.5, Cresset, Litlington, Cambridgeshire, UK; http://www.cresset-group.com/spark/) (Tedesco. 2016). These scores have their own utility where shape score refers to similarity of the obtained molecule to the reference in terms of shape and BIF% refers to percentage similarity to the starter molecule, Score refers to combination of field and shape score while field score refers to similarity of the resultant molecule to the reference in terms of electrostatic and steric field (Tuyishime et al. 2016). In the current study, the above-mentioned approach was implemented. Later, optimized analogues of this maximally explored scaffold were designed that were studied for their possible interactions with anti-fungal targets using network analysis, molecular docking and dynamic analysis.

2.2. Network Analysis

The databases available freely in the public domain provide an immense knowledgebase for the targets and other information pertaining to the chemical moiety. Herein, Ca-DTAR and S-DTAR terminologies were utilized corresponding to drug targets and scaffold target network constructs in *C. albicans*, respectively (Liu, Tu et al. 2018). The physiological or biological pathways (Ca-PW) terminology was utilized to understand the inter-target or inter-indirect target interactions (IP).

2.2.1. Retrieval of the target prediction search data

The search for the protein targets was pursued based on two different aspects. Firstly, a primary network was constructed using all the possible druggable targets of *C. albicans* (Ca-DTAR) (Liu, Tu et al. 2018). While, to construct a network displaying the interactions between that scaffold (2-aminobenzothiazole) and its reported targets (S-DTAR), ChEMBL 24 database was utilized. This database also helped in gathering the information related to bioactivity parameters and medicinal uses. The recent version of this database has around 6 million curated data points for approximately 7500 targets and 1.2 million unique chemicals (https://www.ebi.ac.uk/chembl/) (Gaulton et al., 2017). The information related to gene ID, and gene ontology corresponding to the targets involved

in both the network constructs was retrieved from the Universal Protein Resource (Uniprot) database (https://www.uniprot.org/).

2.2.2. Search for the physiological fungal pathways (Ca-PW)

The above-mentioned networks were further analyzed for the common targets shared among them. These common targets were further searched by their gene IDs for their physiological pathways in *C.albicans* using KEGG database (Kyoto Encyclopedia of Genes and Genomes) (https://www.genome.jp/kegg/) and PANTHER 16 (Protein Analysis THrough Evolutionary Relationships) (http://www.panth erdb.org/). The KEGG displayed pathways in terms of cal (*C.albicans*). While PANTHER shown panther IDs which contains GO annotations term for the molecular and biological processes for the target.

2.2.3. Search for the protein-protein interactions

The STRING database helps to identify the inter protein interactions within the same species (https://string-db.org/). The interactions were classified in terms of direct targets (as the input targets) and the indirect targets (as the associated functional targets) to further understand if the designed molecules may interfere with the normal catalytic activity of other indirect targets by binding to the direct targets. While, searching for the indirect targets corresponding to the selected common targets, some parameters were selected such as text-mining, experimentally reported, neighborhood and co-expression. The results were filtered on the basis of a minimum confidence value of 0.7 (high-confidence) and a maximum number of 30 interaction proteins. The significance of these interactions was scored on the basis of relation between the degrees of a node, betweenness and centrality in the network. The hubs (known with the maximal centrality) and bottleneck (targets associated with hubs as signaling proteins) terms were also studied to understand the mechanism of possible anti-fungal action of the designed 2-aminobenzothiazole based derivatives.

2.2.4. Network Construction

Cytoscape (version 3.8.2, https://cytoscape.org), a freely accessible java-based software, was used for the construction of the network. The results are displayed in cytoscape in the form of a network which is constructed with the help of nodes linked via edge. Herein, the nodes depict the name of the components (fungal name, scaffold name, targets or pathways) and the edges indicates connections between all the nodes. The architecture of the first network is composed of a central fungal name or the scaffold name with surrounding druggable targets (Ca-DTAR and S-DTAR).

On the other hand, the makeup for the second network consists of a central fungal name surrounded with respective concentric circles of S-DTAR, IP and Ca-PW.

2.3. *In-silico* ADMET prediction analysis

To avoid failure of the designed compounds at pre-clinical or clinical stages, a compound should be analyzed for their ADMET properties. To predict these properties for the designed compounds, a freely available ADMET lab 2.0 web-server was utilized (https://admetmesh.scbdd.com/). It uses the SMILE format as the input file for both the designed as well as the standard drugs.

2.4. Molecular Docking

2.4.1. Protein selection and preparation

Prior to the protein preparation, protein selection was carried out by considering the resolution, presence of co-factor, co-crystalized ligand. For each target in the study, the protein structures were selected based on aforementioned criterions. Herein, PDB ID: 5TZ1 for sterol 14-alpha demethylase (*C.albicans*), PDB ID: 1AI9, for Dihydrofolate reductase, PDB ID: 1IYL for N-1myristoryltransferase and PDB ID: 5HUT for trehalose-6 phosphate were selected.

The 3D co-crystallized structures were downloaded from protein data bank (https://www.rcsb.org/) and were further prepared using the flare module of cresset (Cheeseright et al. 2006). The preparation includes the addition of polar hydrogen atoms or missing residues, removal of water molecules and generation of states at pH 7.0±0.5 for the het atoms. Finally, optimization and minimization steps were carried out. This whole preparation was carried using the extensive electron distribution (XED) force field. A grid was created around the active site residues for each of the target proteins reported in the literature.

2.4.2. Ligand preparation

The 3D structures of the designed compounds were imported into flare module of cresset. The obtained structures were optimized and minimized with default settings based on XED force field. The Auto-detect under full protonation mode was used to decipher the .sdf format file.

2.4.3. Docking Simulation

Molecular docking simulations were run on the flare module in Cresset software. The docking scores were calculated with slow but accurate mode. The scoring was obtained in terms of LF Rank Score, LF dG, LF VSscore and LF LE score (Novikov, Stroylov et al. 2012; Ibrahim, Elsaman et al. 2018). Herein, the LF Rank Score indicates the energy ranking for its docked poses and LF dG determines extent of its accurate binding energy towards their target protein. While,

7

LF VSscore describes the virtual screening docking score for the docked protein-ligand complex that narrates the correct rank order for activity in virtual screening. The active ligands are represented with higher negative scores. The LF LE score is based on the ligand efficiency that is best docked (Tomásio, Tedesco et al. ; Stroganov, Novikov et al. 2008; Novikov, Zeifman et al. 2011)

2.5. Electrostatic complementarity (ESC)

ESC analysis assists in calculating detailed map of electrostatic character of ligand and proteins inside the active site. This electrostatic map provides understanding of vital fundamental processes that underline ligand-protein binding which subsequently helps well in drug designing. The ESC was performed on the Spark module of the cresset software; wherein the score come in terms of the EC score (between 0 and 1), here 1 represent complete complementarity and vice-versa. The study was conducted to achieve the three main objectives associated with the docked ligand-target interaction. Firstly, the analysis of charge distribution of a ligand inside the active site. Secondly, the role of the electrostatic potential of ligand that makes it to bind inside target. Lastly, how the change in the binding affinity (based on amino acid interactions) define the favorability as per the effect of substitution on the protein-ligand complex (Bauer and Mackey 2019).

2.6. Molecular Dynamics

To predict the stability of each of the ligand-receptor complexes, a molecular dynamic simulation (MDS) was conducted. The commercially available Flare module from Cresset software uses the OpenMM to comprehend the complex conformational changes and further analyze protein-ligand interaction pattern and their retention throughout the period of dynamics run. The simulation is based on the use of AMBER/GAFF2 force fields in conjunction with AM1-BCC for the charge approach. The initial processing was carried out using water as solvent model. The dimensions were specified for an orthorhombic box having dimension of 10X10X10 Å. Eventually, the final minimization for each docked complex was made upto 0.25 kcal/mol having an equilibrium rate of 200 ps prior to the simulation run. The step size was kept 1 fs and tracked for a time period of 50 ns (Kuhn, Firth-Clark et al. 2020).

2.7. Experimental Section

2.7.1. Chemistry

The chemicals and solvents required for the synthesis were purchased from the Merck, LobaChemie and Avra with purity more than 99%. For analyzing the progress in reactions pre-

8

coated thin layer chromatography (TLC) plates were used (silica gel 60 F254, Merck Millipore). The solvent system comprised of petroleum ether and ethyl acetate. The UV chamber was used for visualizing the plates after the run. The column chromatography technique was implemented for purification of the synthesized compounds. ^{1}H-NMR and ^{13}C-NMR were carried out on BrukerAvance Neo NMR spectrometer at 500MHz and 125 MHz, respectively using CDCl$_3$ as solvent. The chemical shift values (δ) were measured in parts per million (ppm) keeping tetramethylsilane (TMS) as an internal standard. The multiplicity in peaks were observed as a singlet (s), doublet (d), triplet (t), quartet (q), quintet (quin.) and multiplet (m). The coupling constants were calculated in terms of Hertz (Hz) units. The IR spectra were determined using Bruker Alpha ATR spectrometer. The recorded peaks were found to be expressed in cm^{-1}. The HRMS and direct mass spectras were taken from SYNAPT-XS#DBA064 and Waters, Q-TOF Micromass (ESI-MS) spectrometer at positive electrospray ionization (ESI$^+$). The units of peaks recorded are expressed in *m/z* ratio. The melting point (M.pt) of all the synthesized compounds were carried out using oil apparatus.

2.7.2. General procedure for the synthesis of 2-Aminobenzothiazole.

To 10 ml glacial acetic acid in round bottom flask, 10 mmol aniline was added. Followed by addition of 10 mmol potassium isothiocyanate with continuous stirring. To this, a solution of bromine (0.7 ml) in glacial acetic acid (5 ml) was added drop-wise. Reaction was then kept on stirring till its completion is confirmed by TLC. The reaction mixture was then filtered, washed with glacial acetic acid and dried. The obtained crude product was used directly for the next step (Chow et al. 1989; Dalmal et al. 2013; Singh et al. 2020).

2.7.3. General procedure for the synthesis of designed Compounds.

The substituted aromatic acids (1 mmol) were dissolved in 20 ml of dry dichloromethane (DCM) in a round bottom flask and kept for stirring at 0°C. To the solution, 3.33 mmol N, N'-dicyclohexylcarbodiimide (DCC) was added and allowed to stir continuously for an hour. A solution of 1.1 (3.33 mmol) and N, N'-dimethylaminopyridine (DMAP) (0.5 mmol) in DCM (10 ml) was added drop-wise. Stirring was continued for a period of 24 hours. The reaction mixture was analyzed for its completion using pre-coated TLC plates. The reaction mixture was filtered to remove the insoluble N, N'-dicyclohexylurea (DCU) and air dried. The obtained crude product was washed with water (50 ml), 5% acetic acid (50 ml), 1% sodium hydroxide (50 ml) and again with water (50 ml). Followed by washing with brine solution (50 ml), the organic layer was dried

over sodium sulfate and concentrated under vacuum. The purification for the crude dried product was further carried out using the column chromatography (using silica gel #60-120, Pet ether:Ethyl acetate) (**Fig. 3).**
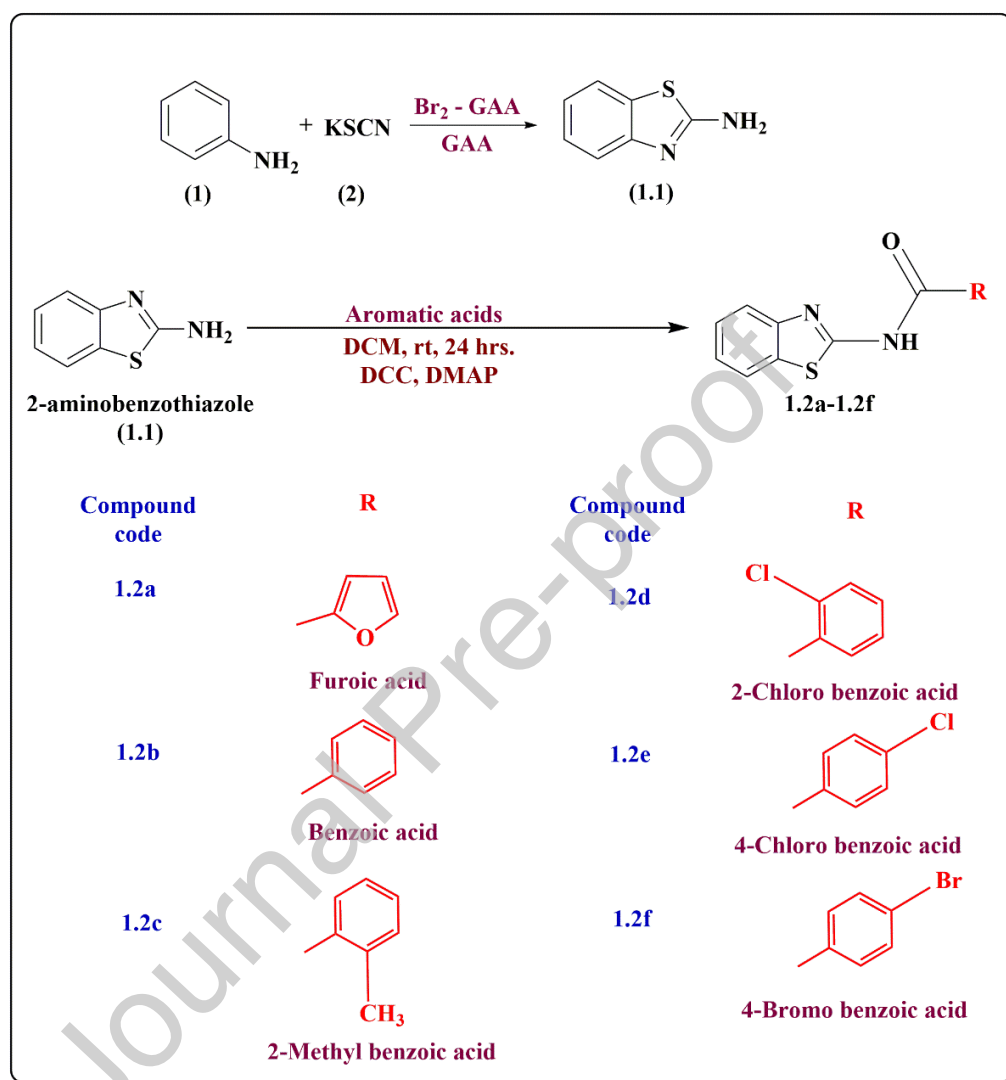
Fig. 3. Synthetic route for the synthesis of designed compounds.

N-(benzo[d]thiazol-2-yl)furan-2-carboxamide (1.2a): white solid powder; yield: 56%; m.p. as 206-210°C; R_f value (Pet ether : Ethyl acetate) as 0.80; m/z for $C_{12}H_8N_2O_2S$ as 245.03[M+H]$^+$; ^{1}H-NMR (500 MHz, CDCl$_3$, δ ppm): 8.1637 (s, 1H$_{10}$), 7.7811-7.7523 (m, 2H$_{4,7}$), 7.5676-7.5379 (m, 3H$_{5,6,15}$), 7.2880-7.2794 (dd, 1H$_{17}$, J=1.6, 0.8Hz), 6.5973-6.5867 (dd, 1H$_{16}$, J=3.6, 1.8Hz); ^{13}C-NMR(125 MHz, CDCl3, δ ppm): 156.03 (C$_{11}$), 147.26 (C$_{15}$), 144.56 (C$_{13}$), 139.19 (C$_2$), 132.09 (C$_{8,9}$), 121.15 (C$_{5,6}$), 118.49 (C$_7$), 116.08 (C$_{17}$), 112.91 (C$_{16}$), 110.81(C$_4$) and FT-IR (KBr, cm^{-1}):

10

C=O (1613), C=C (stretching 1573-1461), =C-H (stretching 2929, 2852), C-O-C (1159), C-N or C=N (1375), C-S (750), N-H (stretching 3475, bending 1573 and wagging 836).

N-(benzo[d]thiazol-2-yl)benzamide (1.2b): white solid powder; yield: 69.04%; m.p. as 190-198°C; R_f value (Pet ether : Ethyl acetate) as 0.73; m/z for $C_{14}H_{10}N_2OS$ as 255.21 $[M+H]^+$; ^{1}H-NMR (500 MHz, CDCl$_3$, δ ppm): 7.9309 (s, 1H$_{10}$), 7.8797-7.8653 (m, 2H$_{14,18}$), 7.7745-7.7582 (m, 2H$_{4,7}$), 7.5877-7.5517 (m, 3H$_{5,6,16}$), 7.5281-7.4997 (m, 2H$_{15,17}$); ^{13}C-NMR(125 MHz, CDCl3, δ ppm): 165.80 (C$_{11}$), 139.72 (C$_2$), 134.31 (C$_{13}$), 132.36 (C$_{16}$), 132.06 (C$_{8,9}$), 128.97 (C$_{15,17}$), 127.06 (C$_{14,18}$), 121.42 (C$_{5,6}$), 118.53 (C$_7$), 110.86 (C$_4$) and FT-IR (KBr, cm^{-1}): C=O (1657), C=C (stretching 1582-1512), C-N or C=N (1395), C-S (712), N-H (stretching 3345, bending 1582 and wagging 828).

N-(benzo[d]thiazol-2-yl)-2-methylbenzamide (1.2c): white solid powder; yield: 71.22%; m.p. as 290-300°C; R_f value (Pet ether : Ethyl acetate) as 0.83; m/z for $C_{14}H_{12}N_2OS$ as 269.01 $[M+H]^+$; ^{1}H-NMR (500 MHz, CDCl$_3$, δ ppm): 7.7297-7.7127 (m, 2H$_{4,7}$), 7.6539 (s, 1H$_{10}$), 7.5559-7.5275 (m, 2H$_{5,6}$), 7.4790-7.4638 (m, 1H$_{14}$), 7.4047-7.3720 (ddd, 1H$_{16}$, J=7.55Hz, 1.3Hz), 7.2921-7.2661 (m, 2H$_{15,17}$), 2.4980 (s, 3H$_{19}$); ^{13}C-NMR(125 MHz, CDCl3, δ ppm): 168.15 (C$_{11}$), 139.78 (C$_2$), 136.70 (), 135.67 (C$_{13}$), 132.11 (C$_{8,9}$), 131.50 (C$_{17}$), 130.76 (), 126.57 (C$_{15}$), 126.03 (C$_{14}$), 121.15 (C$_{5,6}$), 118.48 (C$_7$), 110.85 (C$_4$), 19.74 (C$_{19}$) and FT-IR (KBr, cm^{-1}): C=O (1678), C=C (stretching 1588-1515), =C-H (stretching 2920, 2853), CH$_3$ (bending 1374), C-N or C=N (1374), C-S (738), N-H (stretching 3343, bending 1583 and wagging 818).

N-(benzo[d]thiazol-2-yl)-2-chlorobenzamide (1.2d): white solid powder; yield: 58.06%; m.p. as 201-210°C; R_f value (Pet ether : Ethyl acetate) as 0.65; m/z for $C_{14}H_9ClN_2OS$ as 289.01 $[M+H]^+$; ^{1}H-NMR (500 MHz, CDCl$_3$, δ ppm): 8.0343 (s, 1H$_{10}$), 7.7927-7.7516 (3H$_{4,7,15}$), 7.5747-7.5573 (m, 2H$_{5,6}$), 7.4864-7.4327 (m, 2H$_{16,18}$), 7.4204-7.3880 (m, 1H$_{17}$); ^{13}C-NMR(125 MHz, CDCl3, δ ppm): 164.62 (C$_{11}$), 139.38 (C$_2$), 134.64 (C$_{14}$), 132.10 (C$_{8,9}$), 132.02 (C$_{16}$), 130.62 (C$_{13}$), 130.50 (C$_{15}$), 127.44 (C$_{17,18}$), 121.41 (C$_{5,6}$), 118.86 (C$_7$), 110.77 (C$_4$) and FT-IR (KBr, cm^{-1}): C=O (1665), C=C (stretching 1581-1501), =C-H (stretching 2921, 2852), C-Cl (643), C-N or C=N (1392), C-S (746), N-H (stretching 3317, bending 1581 and wagging 827).

N-(benzo[d]thiazol-2-yl)-4-chlorobenzamide (1.2e): white solid powder; yield: 51.32%; m.p. as 202-212°C; R_f value (Pet ether : Ethyl acetate) as 0.55; m/z for $C_{14}H_9ClN_2OS$ as 289.01 $[M+H]^+$; ^{1}H-NMR (500 MHz, CDCl$_3$, δ ppm): 7.8687 (s, 1H$_{10}$), 7.8265-7.8099 (d, 2H$_{14,18}$, J=8.3Hz), 7.7570-7.7400 (m, 2H$_{4,7}$), 7.5709-7.5539 (m, 2H$_{5,6}$), 7.4969-7.4803 (d, 2H$_{15,17}$, J=8.3Hz); ^{13}C-

NMR(125 MHz, CDCl3, δ ppm): 164.69 (C_{11}), 139.44 (C_2), 138.75 (C_{16}), 132.64 ($C_{8,9}$), 129.25 ($C_{14,18}$), 128.90 ($C_{15,17}$), 128.51 (C_{13}), 121.49 ($C_{5,6}$), 118.87 (C_7), 110.77 (C_4) and FT-IR (KBr, cm^{-1}): C=O (1678), C=C (stretching 1591-1528), =C-H (stretching 2922, 2854), C-Cl (673), C-N or C=N (1396), C-S (747), N-H (stretching 3331, bending 1590 and wagging 829).

N-(benzo[d]thiazol-2-yl)-4-bromobenzamide (1.2f): white solid powder; yield: 43.54%; m.p. as 253-264°C; R_f value (Pet ether : Ethyl acetate) as 0.70; m/z for $C_{14}H_9BrN_2OS$ as 333.44 [M+H]$^+$; ^{1}H-NMR (500 MHz, CDCl$_3$, δ ppm): 7.8667 (s, 1H$_{10}$), 7.7554-7.7395 (m, 4H$_{4,7,14,18}$), 7.6631-7.6460 (m, 3H$_{15,17}$), 7.5736-7.5561 (m, 2H$_{5,6}$); ^{13}C-NMR(125 MHz, CDCl3, δ ppm): 164.69 (C_{11}), 139.44 (C_2), 138.75 (C_{16}), 132.64 ($C_{8,9}$), 129.25 ($C_{14,18}$), 128.90 ($C_{15,17}$), 128.51 (C_{13}), 121.49 ($C_{5,6}$), 118.87 (C_7), 110.77 (C_4) and FT-IR (KBr, cm^{-1}): C=O (1677), C=C (stretching 1590-1500), =C-H (stretching 3029), C-Br (670), C-N or C=N (1395), C-S (746), N-H (stretching 3300, bending 1590 and wagging 829).

## 2.9. Biological evaluation

The synthesized compounds were tested for their in-vitro Anti-fungal activity. The inhibitory effect of these compounds was examined against the fungal species in Microcare laboratories, Surat. The principle of the anti-fungal analysis is based on the use of different dilutions of the test sample which can help to determine the minimum concentration known as the MIC at which there is no visible growth even in the presence of growth media. This quantitative measurements in terms of MIC defines the lowest concentration of the drug substance required to inhibit the 99% of the fungal growth when the minimum inoculum size for the organisms were kept at 10^8 organisms per ml of the dilution. The procurement of the strains used for the anti-fungal activity was done from the Institute of Microbial Technology, Chandigarh. The strain used for the *Candida albicans*, *Aspergillus niger* and *Aspergillus clavatus* were MTCC – 227, MTCC – 282 and MTCC – 1323, respectively. The standards used for the study included the marketed APIs (Fluconazole, Nystatin and Griseofulvin). The MIC value of one of the reference drugs with anti-DFR action i.e., Trimethoprim has been referred from literature (Chan et al. 1995).

3.Results and Discussion

3.1. Lead Identification

Based on the literature survey, there are many 2-aminobenzothiazole derivatives which are maximally explored for anti-fungal activity. Some reported benzothiazole based as anti-fungal

agents are displayed in **Fig.4** along with their respective MIC values. Herein, the lead optimization approach was carried out by selecting the best 2-aminobenzothiazole derivative, (N-(1,3-benzothiazole-2-yl)-2-(pyridine-3-ylformohydrazido) acetamide) (Acharya et al. 2020). This molecule was subjected to bioisosteric replacement to have an effective modification which may improve the anti-fungal activity in comparison to the derivatives reported by Acharya et al., 2020**.** In the current study, major focus was kept on exploring the 2nd position. Prior to search for bioisosteres, molecular mechanism of 2-aminobenzothiazole as anti-fungal was understood by searching for the possible targets and pathways which this scaffold-based derivatives may inhibit or interfer with. To search for possible targets of this scaffold-based derivatives, network analysis was carried out which is discussed in below sections.
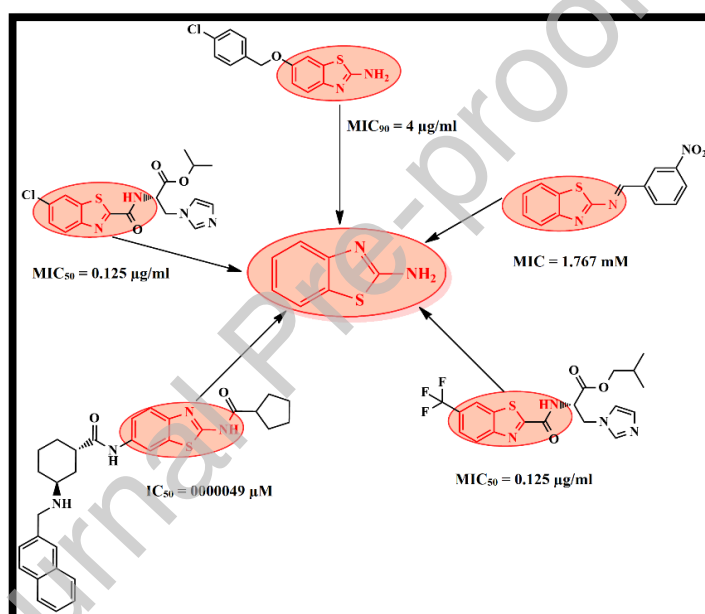
Fig. 4 Structures of the known antifungal agents having the common benzo or 2-aminobenzo thiazole scaffold along with their reported inhibitory activity.

3.2. Target Identification and primary network

The study focused on deciphering the possible anti-fungal targets for the 2-amino benzothiazole based derivatives using network analysis. Therefore, a primary network constituting amalgamation of targets expressed in *C.albicans* fungus with the selected 2-aminobenzothiazole based moiety was constructed. The screening of the common targets was of great significance for developing a secondary network describing the predicted mechanism of action. For this, from the ChemBL database nearly 96 targets were gathered as S-DTAR and from the literature 41 targets were taken

as the Ca-DTAR. All these targets were then confirmed using the gene name from the Uniprot database and are mentioned in **Table 1.** The constructed network using Cytoscape has been displayed in **Fig.5.**

Table 1. The list depicting the common four targets along with their Uniprot ID.

Sr. No.	Common Targets as Gene Name	Protein Name (Uniprot ID)	Reference linked to 2-Aminobenzothiazole
1	ERG11	Lanosterol 14-alpha demethylase (P10613)	(Catalano, Carocci et al. 2013; Zhao, Wei et al. 2018; Djuidje, Sciabica et al. 2020)
2	NMT1	Glycylpeptide N-tetradecanoyltransferase (N-Myrsitosyltransferase P30418)	(Zhao and Ma 2014; Mishra, Ghanavatkar et al. 2019)
3	DFR1	Dihydrofolatereductase (P22906)	(Thakkar, Thakor et al. 2017; Mishra, Ghanavatkar et al. 2019)
4	TPS1	Alpha,alpha-trehalose-phosphate synthase (Trehalose-6-phosphate synthase Q92410)	(Acharya, Jethava et al. 2020)

14
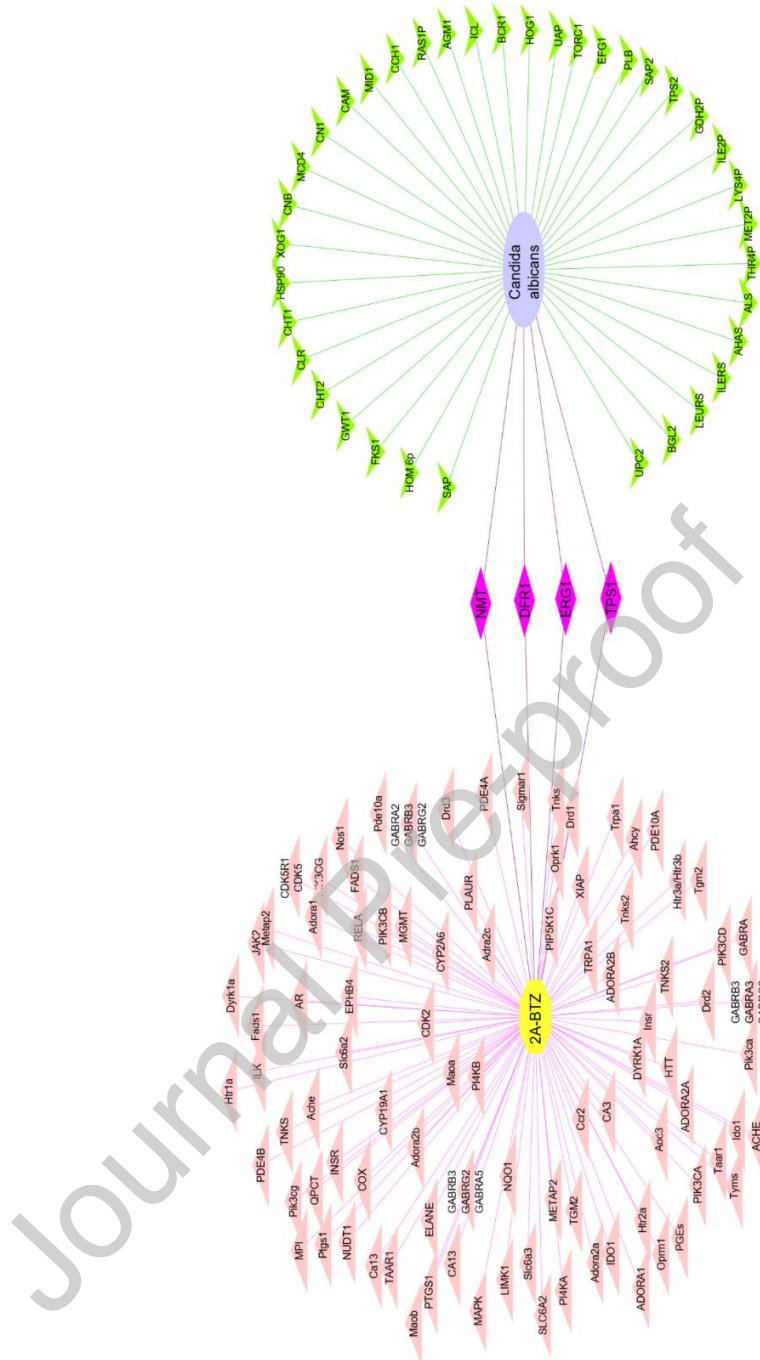
Fig.5 The primary network defining for the protein targets for 2-aminobenzothiazole as S-DTAR (left) and *C. albicans* as Ca-DTAR (right). The central diamonds represent the common targets for the both.

3.3. Searching of the physiological *C.albicans* pathways

15

The common targets previously screened after the primary network were then used to assemble the pathways using the KEGG Pathway module. After a search for biological pathways, a total of 11 Ca-PW that depicts direct participation of the target enzymes ERG11 (Lanosterol 14-α demethylase), DHFR (DihydrofolateReductase) and TPS1 (Trehalose Phosphate 1) were observed. The **table 2** shows all the Ca-PW involved directly with these targets. The pathway for the fourth target NMT1 (N-Mystriryltransferase) was not included in the KEGG. Therefore, gene ontology technique was used to get the functional aspect of the NMT1 in *C.albicans*. Using the PANTHER gene enrichment analysis tool, the search was conducted to find the biological processes though which NMT1 functions inside the fungus. The search revealed that the panther family has a PTHR11377 ID which was found to contain the panther GO-slim biological process, cellular components and molecular functions encoded within the GO-annotation. The functional processes in which the NMT1 was involved were selected. These GO annotations for molecular processes are listed in the **Table 2.**

Table 2. Description of the biological pathways to which the targets belong.

Pathway	Pathway Name	Targets
cal01100	Metabolic Pathways	ERG11, TPS1, DFR1, ERG1-7, ERG9, ERG24-27, PGM2, UGP1, ERG20, NTH1, TPS2, TPS3, GSY1, ADE8, ADE17 and DUT1
cal01110	Biosynthesis of secondary metabolites	ERG11, TPS1, ERG1-7, ERG9, ERG24-27, PGM2, UGP1, ERG20, NTH1, TPS2, TPS3, GSY1, ADE8 and ADE17
cal00100	Steroid biosynthesis	ERG11, ERG1-7, ERG9, ERG24-27 and ERG20
cal00500	Starch and sucrose metabolism	TPS1, TPS2, TPS3, PGM2, UGP1, NTH1 and GSY1
cal00670	One carbon pool by folate	DFR1 and ADE8

cal01240	Biosynthesis of co-factors	DFR1 and UGP1
cal00790	Folate biosynthesis	DFR1 and AKR1
GO:0018193	Peptidyl-amino acid modification	PTHR11377 – NMT1
GO:0006497	Protein lipidation	PTHR11377 – NMT1
GO:0043543	Protein acylation	PTHR11377 – NMT1
cal00230	Purine metabolism	ADE8, ADE17 and PGM2
cal00909	Sesquiterpenoid and triterpenoid biosynthesis	ERG1 and ERG9
cal00520	Amino sugar and nucleotide sugar metabolism	UGP1 and PGM2
cal00052	Galactose metabolism	UGP1 and PGM2
cal04144	Endocytosis	ARF1
cal00730	Thiamine metabolism	THI5
cal04213	Longevity regulating pathway-multiple species	HSP104
cal00010	Glycolysis/Gluconeogenesis	PGM2
cal00030	Pentose phosphate pathway	PGM2
cal00040	Pentose and glucuronateinterconversions	UGP1
cal00240	Pyrimidine metabolism	DUT1

### 3.4. Searching the possible protein-protein interactions

The targets were then probed in the STRING database to visualize the inter-target interactions. At the high confidence level of 0.7 all the target proteins remained un-interacted. The search was then forwarded with few reported parameters. These include the top 30 interacting proteins with 0.7 score for the confidence. The obtained targets were again searched for the *C. albicans* through the KEGG database. The **Table 2.** describes all the targets having their respective candida pathways.

3.5. Construction of a secondary network

The hierarchical distribution required for constructing the network was designed using the layout module from the cytoscape. The network consists of encircled targets (four in this case) over the

17

nucleus, followed by the concentric circles of PPI, gene ontology term and lastly the physiological pathways as shown in **Fig. 6.** The results here depict that the four direct targets that influence 10 biological pathways necessary for the fungal survival. The indirect targets apart from these 10 pathways additionally contribute for 11 other physiological pathways in *C. albicans*.
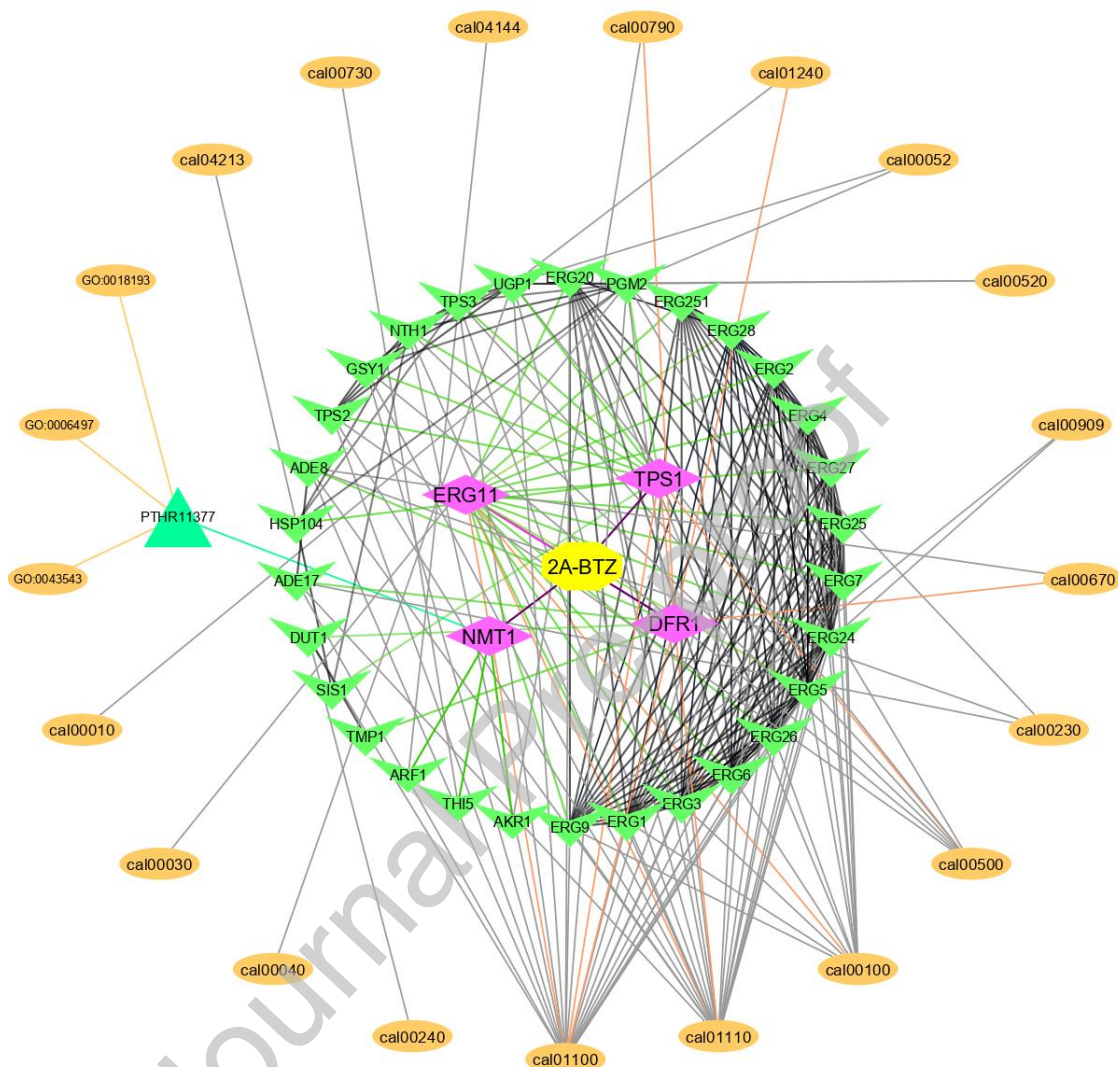
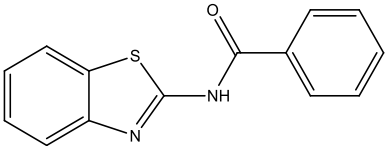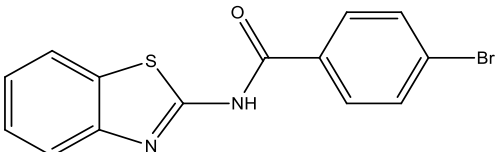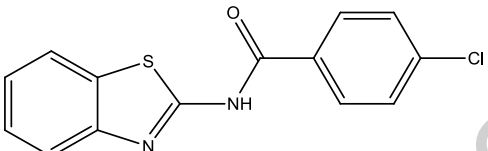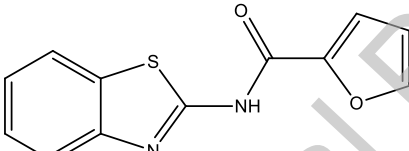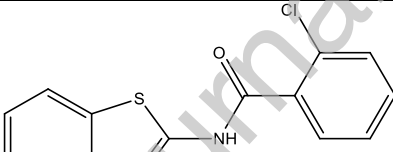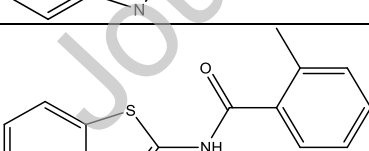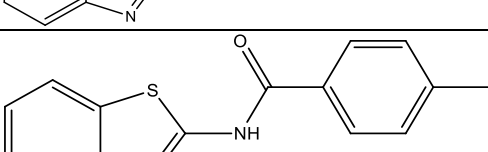**Fig.6** The secondary network consisting of central octagonal shape scaffold, followed by the targets of *C.albicans* in a diamond shape, V and triangle-shaped indirect targets as the PPI and the ellipsoidal shaped physio-chemical pathways.
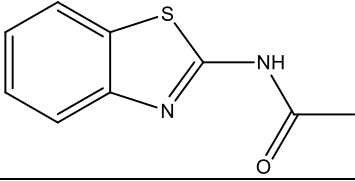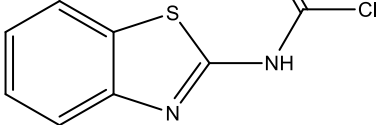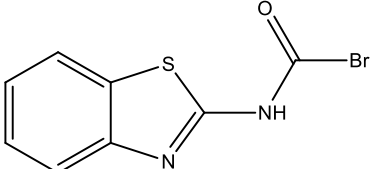
4. Bio-isosteric replacement for lead optimization

As a resultant of the bioisosteric replacement in N-(1,3-benzothiazole-2-yl)-2-(pyridine-3-ylformohydrazido) acetamide, 500 molecules were obtained that may possess similar or improved biological property in comparison to the reference molecule. Among the hits, 2-aminobenzothiazole with benzoyl substitution showed good BIF%, score, field score and shape

score, and was selected for further study. The obtained scores have been displayed in **Table 3**. Based on these scores, different derivatives of 2-aminobenzothiazole were designed and are displayed in **Fig.7**.

Table 3. Top ten hits after Bioisosteric replacement.

Sr. No.	Compound Structure	BIF%[*]	Score[**]	Field Score[***]	Shape Score[****]
1.		77	0.768	0.783	0.753
2.		76	0.760	0.757	0.763
3.		74	0.759	0.756	0.761
4.		72	0.713	0.700	0.726
5.		71	0.711	0.706	0.717
6.		70	0.704	0.704	0.703
7.		70	0.694	0.700	0.688

8.		69	0.689	0.703	0.676
9.		69	0.699	0.686	0.711
10.		68	0.697	0.689	0.706

*(the overall score in percentile, scaled such that no replacement (i.e. just capping with hydrogen)gets a scpre of 0), **(average score for field and steric (shape)), ***(predicted similarity in the electronic fields). ****(predicted similarity in the shape)

As reported that butterfly structure consisting of 2 aryl moieties around the heterocyclic five membered nuclei are biologically stable and active (**Fig. 7.**). Therefore in the current study, based on literature, *in-silico* based designing and synthetic feasibility of the laboratory, the compounds containing the aromatic acid as the substituent were selected for the synthesis. The selected optimized molecules are listed in **Fig.8**.
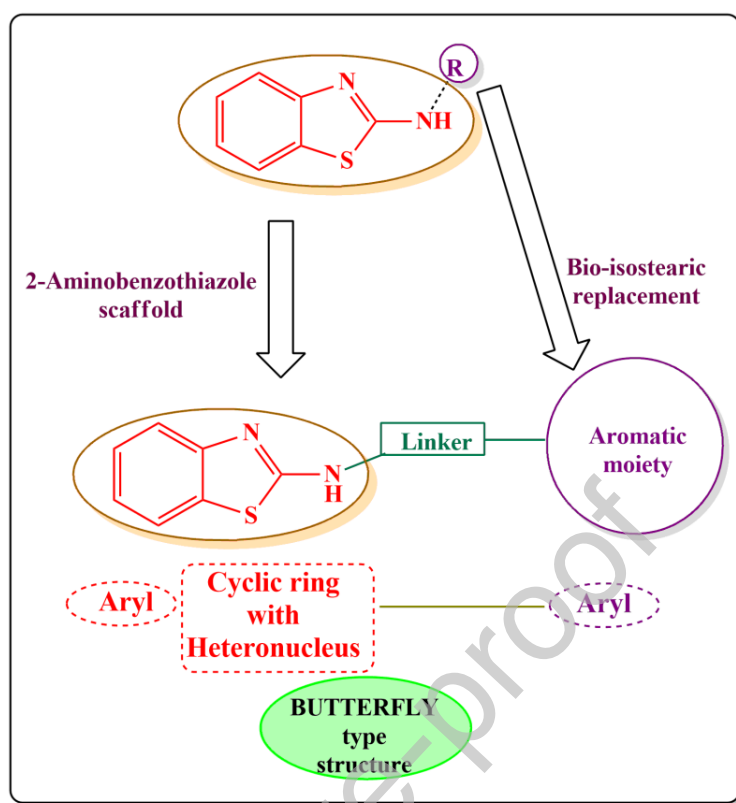
Fig.7 The overall outline for the rationale of the designed molecules.
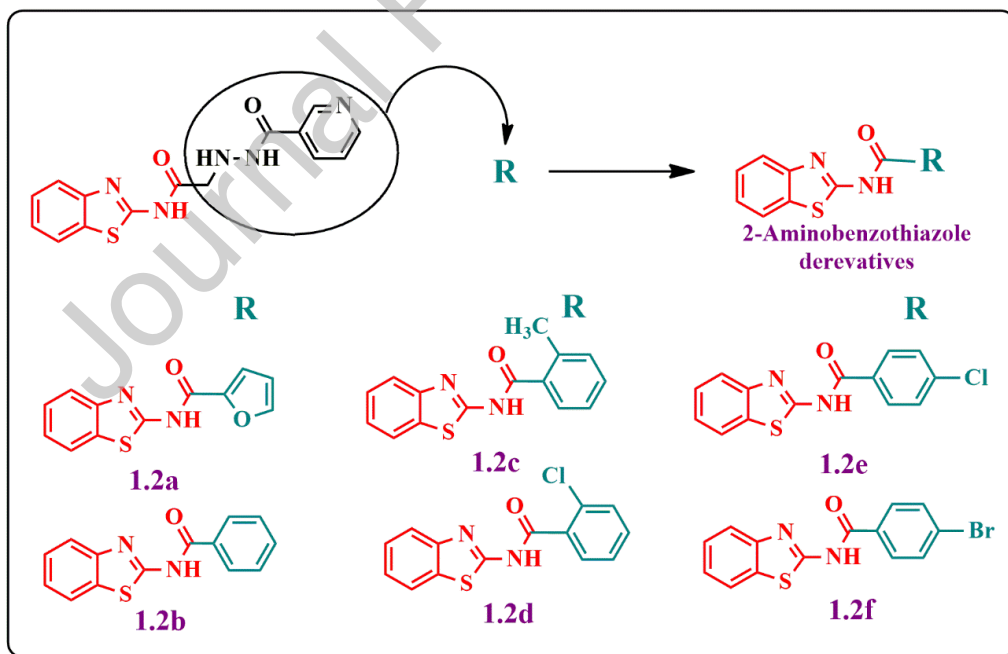
Fig.8 The bioisosteric replacement structure depicting the site of substitution and the list of the designed compounds.

22

5. *In-silico* ADMET prediction

The in-silico prediction of ADMET properties for all the designed molecules indicated that compounds 1.2a to 1.2f falls under the acceptable limits as per the lipinski's rule of five, veber and Ghosh rule. Thereby these designed molecules have drug like properties. All the predicted properties for each of these designed molecules have been displayed in **Table S1**. As per the Lipinski's rule of 5, molecule having MW < 500D, LogP<5, HBA <10 and HBD <5 can only be accepted under the golden triangle.

The other important parameters such as passing blood-brain barrier, VDss (steady state volume of distribution), clearance, half-life and drug induced liver injury were also analyzed to understand if they show these properties comparable to fluconazole, nystatin and griseofulvin. In some instances, the parameters of intermediate Log P, BBB, $T_{1/2}$ or DILI and less MW, nHA or Cl gives an better predicted scores over the most potent anti-fungal medication of fluconazole (**Table S1.**). This result suggests that the designed compounds will have the nearly better ADME profiling. Though the toxic profile of the designed molecule is comparable to fluconazole i.e. may cause hepato-toxicity thereby necessitates to carry further toxicity studies in future.

6. Molecular Docking

To further understand the interaction between designed molecules and the identified targets, docking simulation was carried out. The docking analysis of the designed molecules was carried out in four of the selected targets including CYP51, DHFR, NMT and TPS1. In case of CYP51, most of the designed molecules displayed pi-pi stacking interactions with key residues, Tyr118 and His377 while, displayed sulfur-ion pair interactions with Ser378. In case of 1.2c and 1.2d, some distinct pi-pi interactions were observed with Pro230 and Met508. The essential interactions between the designed ligands and CYP51 enzyme (5TZ1) are displayed in **Fig. S16, Supplementary data.**

In case of DHFR, the designed molecules displayed hydrogen bond interactions with Arg56 and Lys57 while shown cation-pi interactions with Arg79 as shown in **Fig.S17, Supplementary data.** With NMT the designed molecules displayed pi-pi stacking interactions with Tyr225, sulphur-ion pair with Phe339 and pi-pi stacking with Tyr354. As observed in **Fig. S18, Supplementary data.**, additional interactions including pi-pi stacking with Phe115, Tyr225 and Tyr227 were observed. As illustrated in **Fig. S19, Supplementary data,** the interaction pattern for TPS1 (5HUT) were

23

majorly observed to be hydrogen bonding interactions especially with Arg280 and the Lys285**.** The docking scores of each of the designed molecules with the four selected targets have been mentioned in **Table 4**. From **Table 4**, it is clearly indicated that the best scores in terms of LF rank score, LF dG score, LF VSScore and LF LE score were observed for compounds 1.2e and 1.2f.

Table 4. The docking scores for the compounds 1.2a to 1.2f with each target of 5TZ1 (A), 1AI9 (B), 1IYL (C) and 5HUT (D).

| Sr.No.	PDB ID	Compounds	LF Rank score (kcal/mol)	LF dG (kcal/mol)	LF VSscore (kcal/mol)	LF LE (kcal/mol)
A.	5TZ1	1.2a	-9.288	-7.053	-7.626	-0.415
		1.2b	-10.146	-7.348	-8.096	-0.408
		1.2c	-10.114	-7.709	-8.451	-0.406
		1.2d	-10.477	-8.620	-9.128	-0.454
		1.2e	**-10.646**	**-8.343**	**-8.977**	**-0.439**
		1.2f	**-10.252**	**-8.636**	**-9.294**	**-0.455**
B.	1AI9	1.2a	-10.993	-7.063	-7.987	-0.415
		1.2b	-11.409	-7.8	-8.586	-0.433
		1.2c	-11.988	-7.965	-9.179	-0.419
		1.2d	-11.937	-8.552	-9.460	-0.450
		1.2e	**-11.760**	**-8.619**	**-9.291**	**-0.454**
		1.2f	**-11.976**	**-8.886**	**-9.535**	**-0.468**
C.	5HUT	1.2a	-9.412	-6.514	-7.532	-0.383
		1.2b	-9.727	-5.609	-7.029	-0.312
		1.2c	-10.136	-5.650	-7.260	-0.297
		1.2d	-10.388	-6.344	-7.786	-0.334
		1.2e	**-9.176**	**-6.566**	**-7.770**	**-0.346**
		1.2f	**-9.203**	**-6.804**	**-7.896**	**-0.358**
D.	1IYL	1.2a	-11.357	-6.980	-7.738	-0.411
		1.2b	-11.771	-7.852	-8.537	-0.436
		1.2c	-12.224	-8.215	-8.930	-0.432
		1.2d	-12.578	-9.337	-9.774	-0.491
		1.2e	**-12.100**	**-8.527**	**-9.133**	**-0.449**
		1.2f	**-11.712**	**-8.768**	**-9.191**	**-0.461**

7. Electrostatic Complementarity (ESC) for selectivity and SAR analysis

24

To understand the SAR of the designed molecules docked in each of the targets, electrostatic complementarily analysis was carried out. In each of the designed molecules, 2-aminobenzothiazole ring part is common while acid aryl substitution is different. The common part displayed highly complementarity with the key residues of CYP51 only slight clashes were observed at one side of the fused benzothiazole ring. These steric clashes were observed due to the mapping of negative electrostatic potential of Try 118 with this fused benzothiazole ring. Some pi-pi steric clashes at the edge of the aromatic rings of Tyr 132 and fused benzothiazole ring were also observed in each case. Among all the designed compounds, compound 1.2e and 1.2f displayed maximum complementarity. Due to the presence of electron withdrawing groups with –I effect at para position i.e. Cl (1.2e) and Br (1.2f). These group increase the electron density on their surface by withdrawing the electrons from the aromatic ring. This increase in electron density on the surface of the -Cl and -Br group resulted in negative electrostatic potential which were observed to be in complementarity with His377, Tyr64 and Gly65 due to their positive electrostatic potential surface. However, complementarity in 1.2f was less in comparison to 1.2e due to less electronegativity of Br than Cl. In case of other molecules edge aromatic- edge aromatic clashes were observed due to mapping of positive electrostatic potential surface of aryl part on positive electrostatic potential surface of His 377, Tyr 64 and Gly 65.

In case of each of the docked complexes of designed molecules with DFR1, Cl group at para position was found to be favorable in comparison to Cl at ortho position. The strong clashes in compound with Cl at 2nd position were observed due to the mapping of negative electrostatic potential of Cl at 2nd position with negative electrostatic potential of pi-aromatic cloud of Phe 380. While in rest of the part of the compound in 1.2 e and 1.2 f shown high electrostatic complementarity. Similarity Br at para position was also found to be favorable within the active site due to its –I effect though less in comparison to the compound with Cl at para position i.e. 1.2e. In case of 1.2c carbonyl group of amide linkage steric clashed with carbonyl of Ser 378. Similar kind of clashes was observed in case of 1.2d.

In each of the docked complexes of NMT1 and designed compounds, common 2-aminobenzothiazole part shown good complementarity with the enzyme. The steric clashes around the amide linkage in each of the compounds were observed due to its mapping with amino acid Tyr354 bearing positive electrostatic potential. Cl and Br at para position were found to be

25

favorable as they improved the complementarity with the key residues in the active site of NMT1. Highest clashes were observed in compounds 1.2 c and 1.2d especially with Tyr417 and Tyr335. In case of TPS1 1.2 e and 1.2 f shown good complementarity even in this mentioned target, while the rest of the designed compounds shown huge steric clashes with the amino acid residues of TPS1 active site especially in 1.2c and 1.2d. This sort of pattern for the designed compounds was observed in each of the targets indicating 1.2e and 1.2f as the most potential multi-targeted anti-fungal agent.
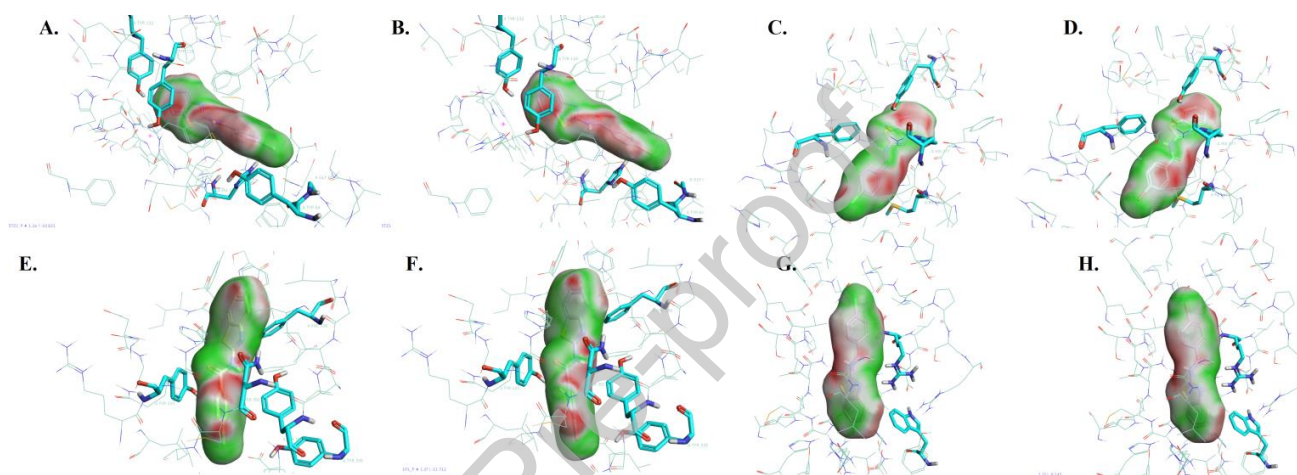
Fig. 9 The electrostatic complementarity surfaces around the ligands complex with selected targets (A) 1.2e-Cyp51 (B) 1.2f-Cyp51 (C) 1.2e-DFR1 (D) 1.2f-DFR1 (E) 1.2e-NMT1 (F) 1.2f-NMT1 (G) 1.2e-TPS1 (H) 1.2f-TPS1
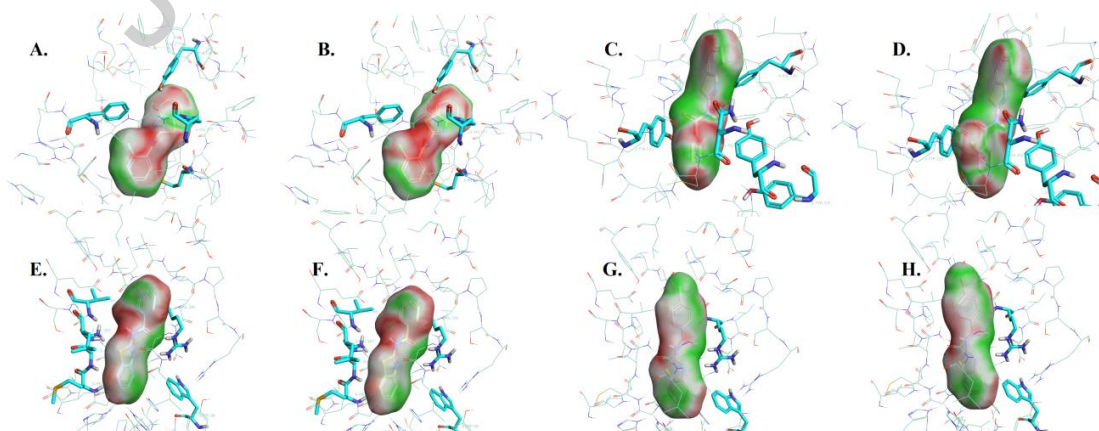
Fig. 10 The electrostatic complementarity surfaces around the ligands complex with selected targets (A) 1.2c-DFR1 (B) 1.2d DFR1 (C) 1.2c-NMT1 (D) 1.2d-NMT1 (E) 1.2a-TPS1 (F) 1.2b-TPS1 (G) 1.2c-TPS1 (H) 1.2d-TPS1

8. Molecular Dynamics Simulation

Each of the docked complexes was analyzed for their stability and retention of docking interactions by molecular dynamic simulations for a period of 50 ns. Overall from the molecular dynamics simulation studies it was observed that most of the docking interactions were retained after the MD simulations. These post-MD interactions can be observed in the **Fig. S20-Fig. S23**. Each of the designed molecules was found to be stable in complex with Cyp51, DFR1 and NMT1 due to minimal RMSD fluctuation i.e. within an acceptable limit of 1Å (**Fig. S24-Fig. S27**). However in case of target TPS1, slight fluctuations were observed initially till 10ns however, regained some stability in later stages of MD. These observed minimal RMSD fluctuations indicates that the designed molecules are stable within the active site cavity of each of the target proteins.

9. Chemistry

The top six compounds were duly synthesized using the two-step reaction. The first step includes synthesis of 2-Aminobenzothiazole via cyclization of aniline with thiocyanate. The second step involved the synthesis of the target compounds via the Steglich reaction of aromatic acid and 2-aminobenzothiazole in the presence of DCC and DMAP using DCM as a solvent. The final compounds were purified using column chromatography and were characterized using IR, ^{1}H-NMR, ^{13}C-NMR and Mass spectrometry. The analysis of the IR spectra suggests the presence of NH stretch between the 3300-3475 cm^{-1} and carbonyl carbon observed around ~1670 cm^{-1}. The ^{1}H-NMR spectra of the synthesized compounds showed broad singlet of NH proton at aδ value ~7.9 ppm. The aromatic protons were found in the range of 7.87 to 7.26 ppm. The compound **1.2c** having methyl substitution showed a singlet for three protons at δ value 2.49 ppm. The ^{13}C-NMR spectra showed that the carbonyl carbon was found to be most downfield and all carbons were found in the range of165.15-110.77 ppm. The carbon of methyl group of the compound **1.2c** showed the peak at a δ value of 19.74 ppm. The results of mass spectrometry showed the molecular ion peak in accordance with the anticipated structures. The analysis of results of spectral characterization suggests that the all compounds were formed and found to be pure.

10. Anti-fungal activity

The synthesized compounds 1.2a to 1.2f were confirmed for their potency in inhibiting growth of fungal micro-organisms through the gold standard (MIC values) evaluation. The inhibitory effect of these compounds was examined against the fungal species by availing the facility from the Microcare laboratories, Surat. The strains used for testing includes the *Candida albicans* (MTCC – 227), *Aspergillus niger* (MTCC – 282) and *Aspergillus clavatus* (MTCC – 1323). The overview of results displayed in **Table 5** indicates that all six compounds were found to manifest exceptional inhibition effect against *C. albicans*, but only good to moderate activity was observed against *Aspergillus* spp. This activity profile obtained against these mentioned strains were compared with known marketed drugs (Fluconazole (oral or I.V.), Nystatin (oral and topical) and Griseofulvin (oral). The analysis is carried out in the form of macro- and micro- dilutions. Specifically for *C. albicans* among all the compounds, 1.2b (100µg/ml) and 1.2e (100µg/ml) exhibited comparable anti-candida activity to Nystatin while superior to Griseofulvin. Both these compounds manifested slightly inferior activity to Trimethoprim and Fluconazole. Meanwhile, another compound 1.2a also lay out a near comparable activity to Nystatin with MIC value of 125µg/ml as shown in Table. The biological MIC values of 1.2c and 1.2f inferred a moderately good response with MIC of 250 µg/ml. Although, the least potent amongst these six compounds was of 1.2d, it still matches its potency levels same as that of Griseofulvin. However, for both the *Aspergillus* species used, the MIC value for anti-fungal level of inhibition varies at different rate as shown in **Table 5**.

Table 5. The enlisted data signify the anti-fungal activities corresponding to the inhibitory MIC (µg/ml) dilution.

Antifungal Activity Table			
Minimal Inhibitory Concentration [µg/ml]			
Test	Compound Code	*C. albicans*	*A. niger*	*A. clavatus*
---	---	---	---	---
1	1.2a	125	500	500
2	1.2b	100	500	1000
3	1.2c	250	1000	500
4	1.2d	500	1000	>1000
5	1.2e	100	250	500
6	1.2f	250	500	500

28

Standard♣	Fluconazole	64	100	100
Standard♣	Nystatin	100	100	100
Standard♣	Griseofulvin	500	100	100
Standard♠	Trimethoprim	>50	-	-

♣ Experimentally calculated MIC value

♠ Reported MIC value (Chan et al. 1995)

The graph was plotted between the MIC concentration (y-axis) and the test compounds on standard drugs (x-axis) to study the response activity for 99% inhibition of the respective fungal species. The activity results have been displayed in a bar graph as shown in **Fig. 11**.
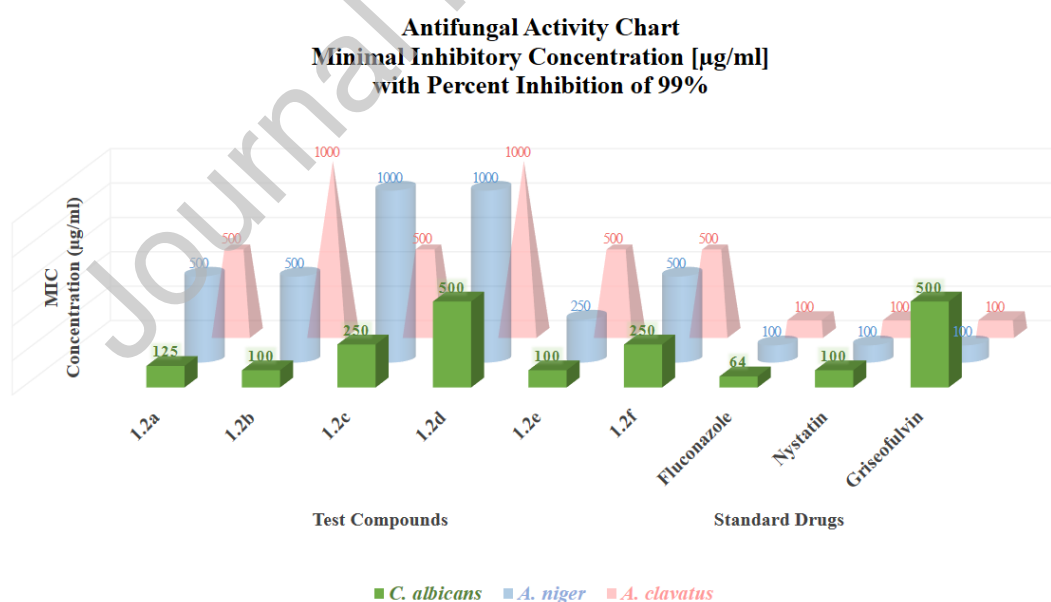
Fig.11. The 3-Dimentional graph representing the anti-fungal activity for all the species along with the standard drugs.

29

Conclusion

Currently, the anti-fungal agents are in great demand especially in ongoing pandemic situation due to growing incidences of fungal infection. 2-aminobenzothiazole is well explored scaffold for designing anti-fungal agents. In the current study, structure of N-(1,3-benzothiazole-2-yl)-2-(pyridine-3-ylformohydrazido) acetamide based molecule was optimized using bioisosteric replacement approach to improve the anti-fungal activity. The possible targets of the designed molecules i.e., Cyp51, DFR1, NMT1 and TPS1 were identified using network analysis. Overall, both in-silico and in-vitro anti-fungal activity suggested that designed compounds (1.2c, 1.2e and 1,2f) were observed to promising anti-fungal compounds. The compounds can further be explored for designing more effective anti-fungal agents using R-group optimization. The study is further open for analyzing thorough pharmacological potential of the designed molecules, experimental pharmacokinetic and toxicity profiling.

Acknowledgement

Disclosure statement

Authors declares no potential conflict of interest.

Author statement

1. Manmeet Singh: Conceptualization, Formal analysis, Methodology, Investigation.
2. Himanshu Verma : Manuscript drafting and editing
3. Priyanka Bhandu: Methodology, Investigation
4. Manoj Kumar: Methodology, Investigation
5. Gera Narendra: Manuscript editing
6. Shalki Choudhary: Manuscript editing
7. Pankaj Kumar Singh: Manuscript editing
8. Om Silakari: Conceptualization, Review, Editing and Supervision
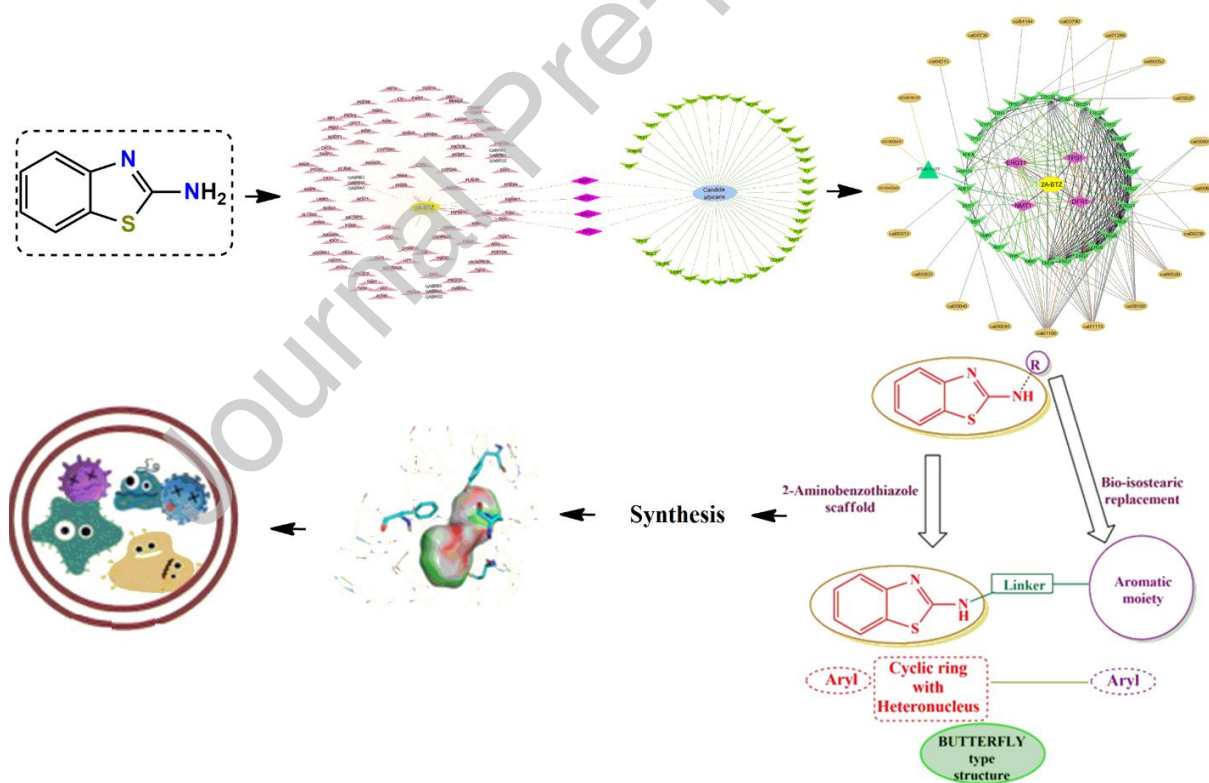
Declaration of interests

NOne

References

Acharya, P.T., Jethava, D.J., Vasava, M.S., Bhavsar, Z.A., Bhoi, M.N., Rajani, D.P. and Patel, H.D., 2020. Synthesis, docking study and biological evaluation of novel N-(1, 3-benzothiazole-2-yl)-2-(pyridine-3-ylformohydrazido) acetamide derivatives.

Al-Nour, M.Y., Ibrahim, M.M. and Elsaman, T., 2019. Ellagic acid, Kaempferol, and Quercetin from Acacia nilotica: Promising combined drug with multiple mechanisms of action. *Current pharmacology reports*, *5*(4), pp.255-280.

Amnerkar, N. D.; Bhongade, B. A.; Bhusari, K. P., Synthesis and biological evaluation of some 4-(6-substituted-1, 3-benzothiazol-2-yl) amino-1, 3-thiazole-2-amines and their Schiff bases. *Arabian Journal of Chemistry* **2015,***8* (4), 545-552.

Bala, R.; Kumari, P.; Sood, S.; Kumar, V.; Singh, N.; Singh, K., Phthaloyl Dichloride–DMF Mediated Synthesis of Benzothiazole-Based 4-Formylpyrazole Derivatives: Studies on Their Antimicrobial and Antioxidant Activities. *Journal of Heterocyclic Chemistry* **2018,***55* (11), 2507-2515.

Bauer, M.R. and Mackey, M.D., 2019. Electrostatic complementarity as a fast and effective tool to optimize binding and selectivity of protein–ligand complexes. *Journal of medicinal chemistry*, *62*(6), pp.3036-3050.

Budha, N.R., Mehrotra, N., Tangallapally, R., Qi, J., Daniels, A.J., Lee, R.E. and Meibohm, B., 2008. Pharmacokinetically-guided lead optimization of nitrofuranylamide anti-tuberculosis agents. *The AAPS journal*, *10*(1), pp.157-165.

Chan, J.H., Hong, J.S., Kuyper, L.F., Baccanari, D.P., Joyner, S.S., Tansik, R.L., Boytos, C.M. and Rudolph, S.K., 1995. Selective inhibitors of Candida albicans dihydrofolate reductase: activity and selectivity of 5-(arylthio)-2, 4-diaminoquinazolines. *Journal of medicinal chemistry*, *38*(18), pp.3608-3616.

Cheeseright, T., Mackey, M., Rose, S. and Vinter, A., 2006. Molecular field extrema as descriptors of biological activity: definition and validation. *Journal of chemical information and modeling*, *46*(2), pp.665-676.

Chu, H., Duan, Y., Lang, S., Jiang, L., Wang, Y., Llorente, C., Liu, J., Mogavero, S., Bosques-Padilla, F., Abraldes, J.G. and Vargas, V., 2020. The Candida albicans exotoxin

candidalysin promotes alcohol-associated liver disease. *Journal of hepatology*, *72*(3), pp.391-400.

Chow, A.W., Bitler, S.P., Penwell, P.E., Osborne, D.J. and Wolfe, J.F., 1989. Synthesis and solution properties of extended chain poly (2, 6-benzothiazole) and poly (2, 5-benzoxazole). *Macromolecules*, *22*(9), pp.3514-3520.

Calderone, R.A. and Fonzi, W.A., 2001. Virulence factors of Candida albicans. *Trends in microbiology*, *9*(7), pp.327-335.

Catalano, A.; Carocci, A.; Defrenza, I.; Muraglia, M.; Carrieri, A.; Van Bambeke, F.; Rosato, A.; Corbo, F.; Franchini, C., 2-Aminobenzothiazole derivatives: search for new antifungal agents. *European Journal of Medicinal Chemistry* **2013**,*64*, 357-364.

Dadmal, T.L., Katre, S.D., Mandewale, M.C. and Kumbhare, R.M., 2018. Contemporary progress in the synthesis and reactions of 2-aminobenzothiazole: a review. *New Journal of Chemistry*, *42*(2), pp.776-797.

Friggeri, Laura, Tatiana Y. Hargrove, Zdzislaw Wawrzak, Anna L. Blobaum, Girish Rachakonda, Craig W. Lindsley, Fernando Villalta et al. "Sterol 14α-Demethylase Structure-Based Design of VNI ((R)-N-(1-(2, 4-Dichlorophenyl)-2-(1 H-imidazol-1-yl) ethyl)-4-(5-phenyl-1, 3, 4-oxadiazol-2-yl) benzamide)) Derivatives to Target Fungal Infections: Synthesis, Biological Evaluation, and Crystallographic Analysis." *Journal of medicinal chemistry* 61, no. 13 (2018): 5679-5691.

Franchini, C., Muraglia, M., Corbo, F., Florio, M.A., Di Mola, A., Rosato, A., Matucci, R., Nesi, M., Van Bambeke, F. and Vitali, C., 2009. Synthesis and biological evaluation of 2-mercapto-1, 3-benzothiazole derivatives with potential antimicrobial activity. *Archiv der Pharmazie: An International Journal Pharmaceutical and Medicinal Chemistry*, *342*(10), pp.605-613.

Gaulton, A., Hersey, A., Nowotka, M., Bento, A.P., Chambers, J., Mendez, D., Mutowo, P., Atkinson, F., Bellis, L.J., Cibrián-Uhalte, E. and Davies, M., 2017. The ChEMBL database in 2017. *Nucleic acids research*, *45*(D1), pp.D945-D954.

Kuhn, M., Firth-Clark, S., Tosco, P., Mey, A.S., Mackey, M. and Michel, J., 2020. Assessment of binding affinity via alchemical free-energy calculations. *Journal of Chemical Information and Modeling*, *60*(6), pp.3120-3130.

Kullberg, B.J. and AM, O.L., 2002. Epidemiology of opportunistic invasive mycoses. *European journal of medical research*, *7*(5), pp.183-191.

Lai, C.C., Wang, C.Y. and Hsueh, P.R., 2020. Co-infections among patients with COVID-19: The need for combination therapy with non-anti-SARS-CoV-2 agents?. *Journal of Microbiology, Immunology and Infection*, *53*(4), pp.505-512.

Liu, N.; Tu, J.; Dong, G.; Wang, Y.; Sheng, C., Emerging new targets for the treatment of resistant fungal infections. *J. Med. Chem.* **2018,***61* (13), 5484-5511.

Lee, P.S., Lapointe, G., Madera, A.M., Simmons, R.L., Xu, W., Yifru, A., Tjandra, M., Karur, S., Rico, A., Thompson, K. and Bojkovic, J., 2018. Application of virtual screening to the identification of new LpxC inhibitor chemotypes, oxazolidinone and isoxazoline. *Journal of medicinal chemistry*, *61*(20), pp.9360-9370.

Lohse, M.B., Gulati, M., Johnson, A.D. and Nobile, C.J., 2018. Development and regulation of single-and multi-species Candida albicans biofilms. *Nature Reviews Microbiology*, *16*(1), pp.19-31.

Novikov, F.N., Stroylov, V.S., Zeifman, A.A., Stroganov, O.V., Kulkov, V. and Chilov, G.G., 2012. Lead Finder docking and virtual screening evaluation with Astex and DUD test sets. *Journal of computer-aided molecular design*, *26*(6), pp.725-735.

Novikov, F.N., Zeifman, A.A., Stroganov, O.V., Stroylov, V.S., Kulkov, V. and Chilov, G.G., 2011. CSAR scoring challenge reveals the need for new concepts in estimating protein–ligand binding affinity. *Journal of chemical information and modeling*, *51*(9), pp.2090-2096.

Pappas, P.G., Rex, J.H., Sobel, J.D., Filler, S.G., Dismukes, W.E., Walsh, T.J. and Edwards, J.E., 2004. Guidelines for treatment of candidiasis. *Clinical infectious diseases*, *38*(2), pp.161-189.

Scordino, F.; Giuffrè, L.; Felice, M. R.; Orlando, M. G.; Medici, M. A.; Merlo, F. M.; Romeo, O., Genetic diversity of Candida albicans isolates recovered from hospital environments and patients with severe acquired brain injuries. *Infect. Genet. Evol.* **2019**, *76*, 104068.

Singh, M., Yadav, L.D.S. and Singh, R.K.P., 2020. Visible-light photoredox catalytic approach for the direct synthesis of 2-aminobenzothiazoles from anilines. *Tetrahedron Letters*, *61*(13), p.151700.

Sheng, C., Zhang, W., Ji, H., Zhang, M., Song, Y., Xu, H., Zhu, J., Miao, Z., Jiang, Q., Yao, J. and Zhou, Y., 2006. Structure-based optimization of azole antifungal agents by CoMFA, CoMSIA, and molecular docking. *Journal of medicinal chemistry*, *49*(8), pp.2512-2525.

Tedesco, G., 2016. Using the Spark reagent databases to identify bioisosteric R-group replacements.

Tomásio, S.; Tedesco, G.; Cheeseright, T., Docking Factor-Xa ligands with Lead Finder.

Tuyishime, M., Lawrence, R. and Cocklin, S., 2016. Core chemotype diversification in the HIV-1 entry inhibitor class using field-based bioisosteric replacement. *Bioorganic & medicinal chemistry letters*, *26*(1), pp.228-234.

Weig, M., Groß, U. and Mühlschlegel, F., 1998. Clinical aspects and pathogenesis of Candida infection. *Trends in microbiology*, *6*(12), pp.468-470.

Wenzel, R.P., 1995. Nosocomial candidemia: risk factors and attributable mortality. *Clinical Infectious Diseases*, *20*(6), pp.1531-1534.

Graphical abstract